Volume 1 | Number 1 | Jan 2013 | Pages 1–100

Dalton Transactions

An international journal of inorganic chemistry
www.rsc.org/dalton

ROYAL SOCIETY
OF CHEMISTRY

This is an *Accepted Manuscript*, which has been through the Royal Society of Chemistry peer review process and has been accepted for publication.

Accepted Manuscripts are published online shortly after acceptance, before technical editing, formatting and proof reading. Using this free service, authors can make their results available to the community, in citable form, before we publish the edited article. We will replace this *Accepted Manuscript* with the edited and formatted *Advance Article* as soon as it is available.

You can find more information about *Accepted Manuscripts* in the **Information for Authors**.

Please note that technical editing may introduce minor changes to the text and/or graphics, which may alter content. The journal's standard **Terms & Conditions** and the **Ethical guidelines** still apply. In no event shall the Royal Society of Chemistry be held responsible for any errors or omissions in this *Accepted Manuscript* or any consequences arising from the use of any information it contains.

ROYAL SOCIETY
OF CHEMISTRY

www.rsc.org/dalton

Journal Name

ARTICLE

Emission energy of azole-based ionic iridium(III) complexes: A theoretical study

Paula Pla,[a] José M. Junquera-Hernández,[a] Henk J. Bolink[a] and Enrique Ortí*[a]

A theoretical density functional theory study has been performed on different families of cationic cyclometallated Ir(III) complexes with general formula $[Ir(C^\wedge N)_2(N^\wedge N)]^+$ and azole-based ligands. The goal was to investigate the effect that the number and position of the nitrogen atoms of the azole ring have on the electronic structure and emission wavelength of the complex. The increase in the number of nitrogen atoms changes the relative energy of the HOMO and LUMO levels and leads to a gradual shift in the emission wavelength that can be larger than 100 nm. The direction of the shift however depends on the ligand in which the azole ring is introduced. The emission shifts to bluer wavelengths when the azole forms part of the cyclometallating C^N ligands, whereas it shifts to the red when the 5-membered ring is incorporated in the ancillary N^N ligand. The position of the nitrogen atoms in the azole ring also plays an important role in determining the emission energy. Complexes with phenyl-azole C^N ligands bearing a nitrogen in the azole position to which the phenyl is linked show a markedly blue-shifted emission compared to complexes with the same number of nitrogen atoms in the azole ring and bearing a carbon atom in that position. Therefore, when comparing the emission properties of azole-based $[Ir(C^\wedge N)_2(N^\wedge N)]+$ complexes, not only the number of nitrogen atoms of the azole but also their position in the ring and the ligand where the azole ring is incorporated should be taken into account.

Introduction

Light-emitting electrochemical cells (LECs) have been widely studied in the last years as promising, low-cost luminescent devices.[1,2] Although the design of LECs is similar to that of organic light-emitting diodes (OLEDs), they present a simpler structure consisting usually in a single layer of an organic semiconductor processed from solution placed between two electrodes. In addition, and in contrast to OLEDs, LECs are not sensitive to the work function of the electrodes, and thus they do not require the use of low work function cathodes that oblige rigorous encapsulation to prevent degradation.[3,4,5]

Ionic transition-metal complexes (iTMCs) are frequently used as the electroactive species in LECs due to their conducting and photoluminescent properties.[6,7] On the one hand, iTMCs are responsible of the charge injection and charge transport processes. The presence of a high concentration of mobile ions in the active layer, able to migrate towards the electrodes when a bias is applied, lowers the injection barriers and allows for a very efficient hole and electron injection.[8,9,10] On the other hand, iTMCs allow for a fine tuning of the emission wavelength by simply modifying the chemical structure of the ligands employed (see ref. 6 and 11 for detailed reports on the many iTMCs studied during the last years). An additional advantage of these materials is the high phosphorescence efficiency they present due to the high spin-orbit coupling induced by the presence of the transition metal.

Within the different phosphorescent iTMCs, cyclometallated iridium(III) complexes are widely employed in LECs because of their thermal stability and the relatively short lifetime of their excited states. Heteroleptic complexes with $[Ir(C^\wedge N)_2(N^\wedge N)]^+$ structure, where C^N is a cyclometallating anionic ligand and N^N an ancillary diimine ligand, are the most promising candidates for the production of stable and long lifetime LECs.[6,12,13,14]

Emission color tuning is achieved by modifying the relative energies of the frontier molecular orbitals, and thus the energy of the emitting excited states. In the $[Ir(C^\wedge N)_2(N^\wedge N)]^+$ complexes, the highest-occupied molecular orbital (HOMO) is predominantly located on the cyclometallating C^N ligands, whereas the lowest-unoccupied molecular orbital (LUMO) is usually centered on the ancillary N^N ligand, as long as it possesses low-lying π* orbitals, as is very often the case.[6] As a consequence, changes in the structure of the cyclometallating ligands mainly alter the HOMO energy, whereas modifications on the ancillary ligand affect the energy of the LUMO.

One of the main interests in the field of electroluminescent devices is to find complexes with emission wavelengths in the blue region of the spectrum, as they are combined with red and green emitting complexes to obtain white-light emitting devices.[15,16,17,18,19,20,21,22,23,24] A simple way to blue-shift the emission wavelength in iTMCs is to increase the HOMO−LUMO gap by modifying the structure of the

cyclometallating ligand to stabilize the HOMO. This can be achieved by introducing electron-withdrawing groups, for example fluorines,[25] or by reducing the ring size of the aromatic N-heterocycle. This second approach presents the advantage of not requiring the formation of $C(sp^2)-F$ bonds, which are very reactive, and can afford instability when the complex is used in LECs.[21,26,27,28]

Concerning the second approach, several examples of Ir(III) complexes with cyclometallating ligands including 5-membered nitrogen-containing rings have been reported, particularly 1-aryl-1,2-pyrazoles,[16,29,30,31,32] and phenyl-imidazoles.[33] Some aryl-triazoles have also been reported (5-aryl-1,2,4-triazoles,[34] and aryl-1,2,3-triazoles.[35,36,37,38,39,40]) and a few aryl-tetrazoles.[41] However, the experimental values recorded for the emission wavelengths of these complexes do not completely fit the expected trend that the emission energy increases with the number of nitrogen atoms. Taking the archetype complex $[Ir(ppy)_2(bpy)]^+$ (Hppy = 2-phenylpyridine, bpy = 2,2'-bipyridine) with emission maximum (λ_{max}) at 585 nm as a reference,[12] the analogous pyrazole complex $[Ir(ppz)_2(bpy)]^+$ (Hppz = 1-phenyl-1,2-pyrazole) shows a significant blue shift with λ_{max} = 563 nm.[29] In contrast, the triazole complex $[Ir(phtl)_2(bpy)]^+$ (Hphtl = 4-phenyl-1-benzyl-1,2,3-triazole), featuring a λ_{max} of 580 nm,[36] is less shifted to the blue than the pyrazole complex, in spite of the higher number of nitrogen atoms that involves the azole ring. The tetrazole complex $[Ir(ptrz)_2(bpy)]^+$ (Hptrz = 2-methyl-5-phenyl-$2H$-tetrazole) exhibits a largely blue-shifted emission with λ_{max} of 545 nm.[41] These experimental results seem to indicate that an increase of the number of nitrogen atoms in the 5-membered heterocycle does not warrant an increase of the emission energy of the complex, although one might expect that the presence of electron-rich nitrogen atoms in the C^N ligands should proportionally enhance the ligand field splitting of Ir(d) orbitals.

In this work, we investigate the electronic properties of $[Ir(C\text{^}N)_2(N\text{^}N)]^+$ complexes incorporating azole rings in the C^N and N^N ligands with the aid of quantum-chemistry calculations. The main goal of the study is to systematize the effect that the number of nitrogen atoms forming the azole ring has on the emission properties. To do so, both the energy and topology of the frontier molecular orbitals (HOMOs and LUMOs) and the nature and relative energy of the lowest-lying triplet electronic states of the complexes are analyzed, and the results are compared with those of the reference complex $[Ir(ppy)_2(bpy)]^+$ (**1**). The complexes included in the first part of the study are those depicted in Chart 1, which include an increasing number of nitrogen atoms in the five-membered ring of the C^N ligand. Complexes with 2, 3 and 4 nitrogen atoms in the azole ring are denoted as **a**, **b** and **c**, respectively. To investigate the relevance of the azole position in which the nitrogen atoms are placed, the electronic properties obtained for the series of complexes **2a-c** are compared with those calculated for complexes **3a-c**. The main difference between these two families is the nature of the atom to which the phenyl substituent is linked: a nitrogen atom for **2a-c** and a carbon atom for **3a-c**. The effect of adding nitrogen atoms in the ancillary N^N ligand is studied in the second part of the study by calculating the electronic properties of complexes **4a-c**, for which an azole-based N^N ligand is used in combination with ppy⁻ as the C^N ligand (Chart 2).

Due to the differences in the structure of the ligands and the number of nitrogen atoms, the numbering of the positions in the five-membered azole ring changes between complexes. To

simplify the discussion, a fixed numbering, starting from the coordinated nitrogen atom, is assigned to each position of the five-membered ring as indicated in Scheme 1.
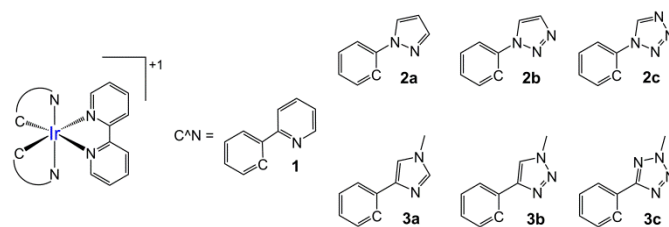
Chart 1 Ionic Ir(III) complexes with an increasing number of nitrogen atoms in the phenyl-azole cyclometallating C^N ligand.
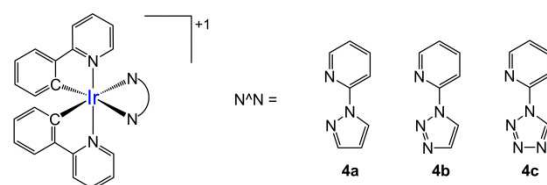
Chart 2 Ionic Ir(III) complexes with an increasing number of nitrogen atoms in the pyridine-azole ancillary N^N ligand.
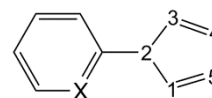
Scheme 1 Labelling used to design the positions of the five-membered ring in phenyl-azole (X = C) cyclometallating and pyridine-azole (X = N) ancillary ligands.

Computational Details

Density functional calculations (DFT) were carried out with the D.01 revision of the Gaussian 09 program package[42] using Becke's three-parameter B3LYP exchange-correlation functional[43,44] together with the 6-31G** basis set for C, H and N,[45] and the "double-ζ" quality LANL2DZ basis set for the Ir element.[46] An effective core potential (ECP) replaces the inner core electrons of Ir leaving the outer core $[(5s)^2(5p)^6]$ electrons and the $(5d)^6$ valence electrons of the Ir(III). The geometries of the singlet ground state and of the lowest-energy triplet state were fully optimized for all complexes without imposing any symmetry restriction. The geometries of the triplet states were calculated using the spin unrestricted UB3LYP approach with a spin multiplicity of 3. The expectation values calculated for S^2 were always smaller than 2.05. All the calculations were performed in the presence of the solvent (acetonitrile). Solvent effects were considered within the self-consistent reaction field (SCRF) theory using the polarized continuum model (PCM)[47,48,49] approach. Phosphorescent emission energies were estimated as the vertical energy difference between T_1 and S_0 at the optimized minimum-energy geometry of T_1. The calculation of the energy of S_0 at the T_1 geometry was performed as an equilibrium single-point calculation with respect to the solvent reaction field/solute electronic density polarization process.. Time-dependent DFT (TD-DFT) calculations of the lowest-lying 20 triplets were performed in the presence of the solvent at the minimum-energy geometry optimized for the ground state.

Results and discussion

Adding nitrogen atoms to the cyclometallating ligands

The molecular and electronic structures of the complexes depicted in Chart 1 were investigated by a combined DFT/TD-DFT study at the B3LYP/(6-31G**+LANL2DZ) level in the presence of the solvent. The geometry of the complexes in their electronic ground state (S_0) was first optimized. Previous theoretical studies on similar systems have shown that the B3LYP/(6-31G**+LANL2DZ) approach reproduce accurately the experimental X-ray geometries slightly overestimating the Ir(III) coordination distances.[12,41,50] The calculations performed on complexes **1**, **2** and **3** show that, in all cases, both the cyclometallating and the ancillary ligands are close to planar (the angle between the planes of the two rings being around 1º) and define a near-octahedral coordination for the Ir metal as is usually observed for this type of complexes.[12,32,41,51,52] The bite angle formed by the phenyl-azole C^N ligands in complexes **2** and **3** is always around 80º, and is similar to that defined by the ppy ligand in **1** (81º).

Fig. 1 shows the energy and the electron density contours calculated for the HOMO and LUMO of complexes **2a-c** and includes complex **1** as a reference system. The atomic orbital composition of the frontier MOs is very similar for all the complexes, and fits the expected behavior for this kind of compounds. The HOMO is mainly composed of a mixture of Ir(III) d_π orbitals and phenyl π orbitals of the cyclometallating ligands, with no contribution from orbitals of the ancillary ligand. In contrast, the LUMO corresponds to the π^* LUMO of the bipyridine ligand with a very small contribution from the metal, and show no participation of the main ligands. Compared to **1**, the substitution of the pyridine ring in the C^N ligands by an azole leads to a stabilization of the HOMO, which decreases in energy gradually as the number of nitrogen atoms in the azole ring increases. The stabilization of the HOMO amounts to 0.65 eV in passing from **1** to **2c**. The energy of the LUMO also experiences a slight stabilization, decreasing in 0.12 eV from **1** to **2c**. The higher stabilization effect predicted for the HOMO is an expected result, because this orbital mostly resides on the C^N ligands and the structural differences in the **2a-c** series rely on these ligands. An increase in the HOMO−LUMO gap is therefore computed along the series **1** (3.22 eV) < **2a** (3.31 eV) < **2b** (3.59 eV) < **2c** (3.75 eV). This trend suggests that the excited state originating in the HOMO−LUMO excitation will appear at higher energies as the number of nitrogen atoms in the azole ring increases in the **2a-c** series.
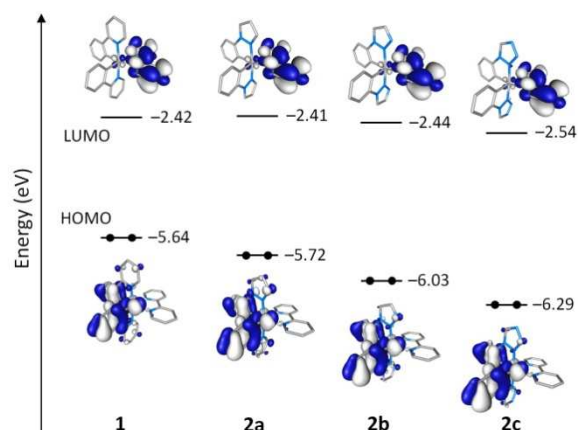
Fig. 1 Schematic representation showing the isovalue contours (±0.03 a.u.) and the energies calculated for the frontier molecular orbitals of complexes **1** and **2a-c**. Hydrogen atoms are omitted.

To investigate the nature of the lowest-energy triplet excited states, a TD-DFT study was performed for each complex at the optimized geometry of S_0. Table 1 summarizes the excitation energy and the electronic description computed for the first triplet states of **1** and **2a-c**. For all the four systems, the lowest-lying triplet (T_1) mainly results from the HOMO → LUMO excitation and therefore implies a charge transfer from the metal and the cyclometallating ligands environment, where the HOMO is located, to the ancillary ligand, where the LUMO resides (see Fig. 1). The T_1 state therefore shows a mixed metal-to-ligand/ligand-to-ligand charge transfer (MLCT/LLCT) character. For **2c**, T_1 shows a larger multiconfigurational character at the TD-DFT level due to its proximity to higher excited states, and the HOMO → LUMO excitation only represents the 41% of the wave function. Nevertheless, the MLCT/LLCT character of T_1 is also confirmed for **2c** as discussed below. The energy of T_1 increases gradually in passing from **1** (2.50 eV) to **2c** (3.04 eV), in good agreement with the trend calculated for the HOMO−LUMO gap. It is of interest to compare this evolution with that calculated for the first ligand-centered (LC) triplet state located on the ancillary bpy ligand (T_4 for **1** and T_2 for **2a-c**, Table 1). The energy of this state remains mostly constant (2.96 to 3.05 eV) because it mainly implies MOs that involve the ancillary ligand, and it becomes mostly degenerate with the MLCT/LLCT T_1 state for complex **2c**.

Table 1 Lowest triplet excited states calculated at the TD-DFT B3LYP/(6-31G**+LANL2DZ) level for complexes **1** and **2a-c** in acetonitrile solution. Vertical excitation energies (E), dominant monoexcitations with contributions (within parentheses) greater than 20% and description of the excited state are summarized. H and L denote HOMO and LUMO, respectively.

Complex	State	E (eV)	Monoexcitations	Description
1	T_1	2.50	H → L (98)	^{3}MLCT/^{3}LLCT
	T_2	2.77	H → L+1 (66)	^{3}LC/^{3}MLCT
	T_3	2.81	H → L+2 (54)	^{3}LC/^{3}MLCT
			H–1 → L+1 (26)	^{3}LC/^{3}MLCT
	T_4	2.96	H–2 → L (36)	^{3}MLCT/^{3}LLCT
			H–6 → L (34)	^{3}LC^a
2a	T_1	2.60	H → L (98)	^{3}MLCT/^{3}LLCT

	T_2	2.95	H–2 → L (52)	^{3}MLCT/^{3}LLCT
			H–6 → L (34)	^{3}LC^a
2b	T_1	2.88	H → L (98)	^{3}MLCT/^{3}LLCT
	T_2	3.03	H–6 → L (55)	^{3}LC^a
			H–2 → L (20)	^{3}MLCT/^{3}LLCT
2c	T_1	3.04	H → L (41)	^{3}MLCT/^{3}LLCT
			H → L+1 (34)	^{3}LC
	T_2	3.05	H–4 → L (41)	^{3}LC/^{3}MLCT
			H–6 → L (32)	^{3}LC^a

^{a} The H–6 → L monoexcitation corresponds to a π→π* transition fully centered on the ancillary N^N ligand.

The MLCT/LLCT nature and low energy of the HOMO → LUMO T_1 triplet suggest that it very likely corresponds to the state from which phosphorescent emission takes place. The great contribution of the metal to this state induces a relevant spin-orbit coupling that allows the otherwise spin-forbidden transition to S_0. A significant blue-shift of the emission wavelength is therefore to be expected along the series **1**, **2a**, **2b** and **2c**.

To get additional information about the emitting state, the geometry of the lowest-energy triplet excited state T_1 was fully optimized using the spin-unrestricted UB3LYP approach. The phosphorescent emission energy was then estimated as the vertical energy difference between T_1 and S_0 at the optimized minimum-energy geometry of T_1 (E_{em} in Fig. 2). The results obtained are summarized in Fig. 2, together with the unpaired-electron spin density distributions calculated for the lowest-energy triplet of complexes **1** and **2a-c**. The spin density distribution presents the same shape for the four complexes (Ir ~ 0.5e, C^N ligands ~ 0.5e, N^N ligand ~ 1.0e) and perfectly matches the topology of the HOMO → LUMO excitation. It confirms the electron transfer from the Ir(C^N)$_2$ environment to the ancillary ligand and, therefore, the ^{3}MLCT/^{3}LLCT character of the T_1 state. The values calculated for E_{em} predict a gradual blue shift along the series **1** (2.07 eV) < **2a** (2.15 eV) < **2b** (2.42 eV) < **2c** (2.57), in good agreement with the evolution of the HOMO−LUMO gap and the TD-DFT excitation energies discussed above. The E_{em} values are in good correlation with the available λ_{em} experimental data (Fig. 2), which gives support to the reliability of the theoretical results.
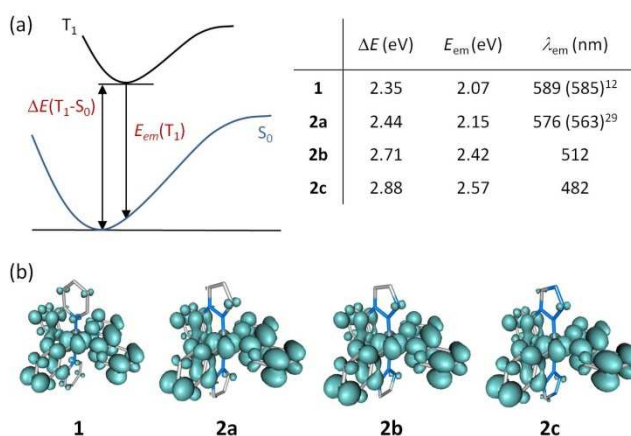
Fig. 2 a) Schematic energy diagram showing the adiabatic energy difference (ΔE) between S_0 and T_1 and the emission energy (E_{em}) from T_1 computed for complexes **1**, **2a**, **2b** and **2c**. Experimental λ_{em} values at 298 K are given within

parentheses for **1**[12] and **2a**.[29] b) Unpaired-electron spin density contours (0.002 au) calculated for the fully relaxed T_1 state.

According to the theoretical results, complexes **2a**, **2b** and **2c** therefore behave following chemical intuition in the sense that as the number of nitrogen atoms in the azole ring increases the HOMO−LUMO gap enlarges and the emission energy gradually shifts to the blue. However, this trend does not explain the anomalous behavior observed experimentally for the triazole complex [Ir(phtl)$_2$(bpy)]$^+$ that remains unsettled. As discussed above, the emission of [Ir(phtl)$_2$(bpy)]$^+$ (580 nm)[36] is red-shifted compared to the pyrazole complex **2a** (563 nm),[29] and is far from that predicted here for the triazole complex **2b** (512 nm). Let us point that there is a significant difference between the [Ir(phtl)$_2$(bpy)]$^+$ complex and **2b**: in the former, the position linking the azole ring to the phenyl substituent (position 2 in Scheme 1) is occupied by a carbon atom, whereas this position is occupied by a nitrogen atom in **2b**. To disentangle the relevance of this structural difference, a comparative study was performed on complexes **3a-c**, which mainly differ from **2a-c** in that position 2 of the azole is occupied by a carbon atom instead of a nitrogen atom (see Chart 1).

Fig. 3 displays the frontier MOs calculated at the optimized minimum-energy geometry of S_0 for complexes **3a-c**, together with those of the reference complex **1**. The topology of the MOs is identical to that of **2a-c** (Fig. 1), but the HOMO appears ~0.4 eV higher in energy than in complexes **2a-c** with the same number of nitrogen atoms in the azole ring. The LUMO is also destabilized but in a smaller amount (~0.10 eV) because it mainly resides on the ancillary ligand where no structural change is made. For **3a** the energy of both MOs is indeed above the corresponding MOs of the reference complex. This result indicates that the energy stabilization produced by the inclusion of a second nitrogen atom in the five-membered ring of the C^N ligand, in a position other than that linking the azole to the phenyl ring, is not compensating the destabilization induced by the reduction of the ring size. This effect is more important in the HOMO due to the higher contribution of the main ligands where the structural modification is performed. As a consequence, **3a** presents a HOMO−LUMO gap (3.02 eV) smaller than those calculated for **1** (3.22 eV) and **2a** (3.31 eV).

The inclusion of additional nitrogen atoms in the azole ring has the same effect reported for the **2a-c** series, and the HOMO−LUMO gap increases (**3a**: 3.02 eV; **3b**: 3.29 eV; **3c**: 3.50 eV) as the number of nitrogen atoms does. However, as the starting point is a smaller HOMO−LUMO gap for the diazole-based complex **3a**, the gaps calculated for complexes **3a-c** are significantly smaller −by about 0.3 eV− than those found for the corresponding **2a-c** complexes. This suggests that emission in **3a-c** has to be expected to be red-shifted with respect to **2a-c**, and would not necessarily appear at higher energies compared to **1**.

Dalton Transactions Accepted Manuscript
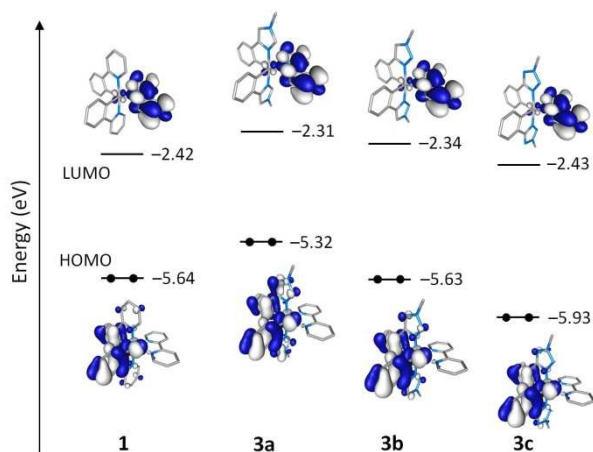
Fig. 3 Schematic representation showing the isovalue contours (±0.03 a.u.) and energies calculated for the frontier molecular orbitals of complexes **1** and **3a-c**. Hydrogen atoms are omitted.

TD-DFT calculations (Table 2) confirm the trends inferred from the evolution of the HOMO−LUMO gap. The first triplet excited state of **3a-c** results from the HOMO → LUMO excitation and is computed at lower energies (~0.3 eV) than the respective triplet in complexes **2a-c**. The T_1 state therefore has a mixed MLCT/LLCT character and increases in energy along the series **3a** (2.32 eV) < **3b** (2.58 eV) < **3c** (2.79 eV) as found for **2a-c**. The LC triplet located on the ancillary ligand remains at similar energies than in **2a-c** between 2.90 and 3.02 eV.

Table 2 Lowest triplet excited states calculated at the TD-DFT B3LYP/(6-31G**+LANL2DZ) level for complexes **3a-c** in acetonitrile solution. Vertical excitation energies (E), dominant monoexcitations with contributions (within parentheses) greater than 20% and description of the excited state are summarized. H and L denote HOMO and LUMO, respectively.

Complex	State	E (eV)	Monoexcitations	Description
3a	T_1	2.32	H → L (98)	^{3}MLCT/^{3}LLCT
	T_2	2.79	H−2 → L (70)	^{3}MLCT/^{3}LLCT
	T_3	2.90	H−4 → L (87)	^{3}LC^a
3b	T_1	2.58	H → L (98)	^{3}MLCT/^{3}LLCT
	T_2	2.97	H−6 → L (39)	^{3}LC^a
			H−2 → L (23)	^{3}MLCT/^{3}LLCT
			H−4 → L (22)	^{3}MLCT/^{3}LLCT
3c	T_1	2.79	H → L (98)	^{3}MLCT/^{3}LLCT
	T_2	3.02	H−6 → L (46)	^{3}LC^a

^{a} The monoexcitation is fully centered on the ancillary N^N ligand.

The T_1 state of complexes **3a-c** was further investigated by fully optimizing its geometry at the UB3LYP level. These calculations confirm the HOMO → LUMO MLCT/LLCT character of T_1 and provide the emission energies listed in Table 3. The estimated E_{em} values are red-shifted with respect to those of the **2a-c** series by ~0.25 eV, and are in good agreement with the available experimental values. The emission wavelength calculated for the triazole complex **3b** (575 nm) is very close to that experimentally observed for [Ir(phtl)$_2$(bpy)]$^+$ (580 nm)[36] and explains the apparently anomalous behavior of this complex that shows almost no blue shift compared with **1** (585 nm).[12]

Table 3 Adiabatic energy difference (ΔE) between S_0 and T_1 and emission energy (E_{em} and λ_{em}) from T_1 computed for complexes **3a-c** Experimental values at 298K are given within parentheses.

Complex	ΔE (eV)	E_{em} (eV)	λ_{em} (nm)^a
3a	2.17	1.91	649
3b	2.43	2.16	575 (580)^{36,b}
3c	2.63	2.35	528 (545)^{41}

^{a} Experimental values at 298K are given within parentheses. ^{b} Experimental value for [Ir(phtl)$_2$(bpy)]$^+$.

In summary, two different effects arise from the emission energies calculated for complexes **2a-c** and **3a-c**. First, an increase in the number of nitrogen atoms in the azole ring of the cyclometallating C^N ligand leads to an increase in the HOMO−LUMO energy gap and to a blue-shift of the emission wavelength. Second, those complexes in which position 2 of the azole ring is occupied by a carbon atom, as in **3a-c**, present a decrease in the HOMO−LUMO energy gap and a red-shift of the emission wavelength with respect to the equivalent complexes with the same number of nitrogen atoms in the azole ring in which there is a nitrogen in position 2 (**2a-c**). The available experimental values correspond to the complexes [Ir(ppz)$_2$(bpy)]$^+$ or **2a** (563 nm),[29] [Ir(phtl)$_2$(bpy)]$^+$ (580 nm)[36] and [Ir(ptrz)$_2$(bpy)]$^+$ or **3c** (545 nm).[40] These complexes actually form a mixed family where one member, the pyrazole-based **2a,** has a nitrogen atom in position 2 of the azole ring, and two members, the triazole [Ir(phtl)$_2$(bpy)]$^+$ complex analogous to **3b** and the tetrazole-based **3c**, have a carbon atom in position 2. For **3b**, and consequently for [Ir(phtl)$_2$(bpy)]$^+$, the reported effects of increasing the number of nitrogen atoms and the presence of a carbon atom in position 2 of the azole compensate each other, and the emission wavelength is even higher than that calculated for **2a**. The initial analysis of the experimental values did not take into account the second effect ignoring the relevance of the atom occupying position 2 in the azole ring. Thus, the observation that could be taken from the experimental results, that the increase in the number of nitrogen atoms in the azole ring did not guarantee a blue shift in the emission wavelength, was wrong. According to our results, the increase in the number of nitrogen atoms always induces the expected blue shift, as long as a coherent structural group of complexes in which no other factor influences the frontier MOs energies and the HOMO−LUMO gap is studied.
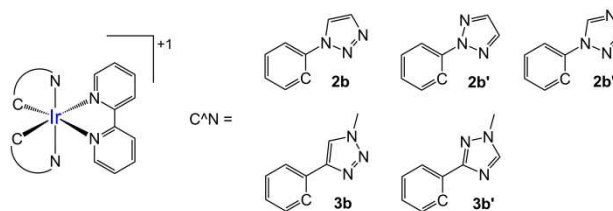
Chart 3 Ionic Ir(III) complexes derived from **2b** and **3b** by changing the position of one nitrogen atom in the azole ring.

A new question arises from the previous discussion about how important is the position occupied by nitrogen atoms in positions other than 1 (the coordination position) and 2 (the phenyl position) and its influence on the emission energy of the complex. To address this question, a new set of triazole-based complexes was studied (Chart 3), in which the position of the third nitrogen atom of the azole ring is changed with respect to

the initial complexes **2b** and **3b**. Table 4 summarizes the results obtained for the new complexes after performing a set of calculations analogue to those previously discussed for **2a-c** and **3a-c**. Moving a nitrogen from position 5 to position 3 to obtain complexes **2b'** and **3b'** induces a small decrease in the HOMO−LUMO gap (0.10 and 0.02 eV, respectively) and a red shift in the expected emission wavelength that is more accentuated for **2b'** (20 nm) than for **3b'** (7 nm). Both changes are much smaller than those observed when we go from **2b** to **3b** (63 nm) or from **2b'** to **3b'** (50 nm) moving the nitrogen atom out of position 2. The results obtained for **2b'** and **2b''** are quite similar, indicating that placing the third nitrogen atom at positions 3 or 4 is nearly equivalent.

Table 4 HOMO and LUMO energies, HOMO−LUMO gap (ΔE_{H-L}), adiabatic energy difference (ΔE) between S_0 and T_1 and emission energy (E_{em} and λ_{em}) from T_1 computed for complexes **2b** and **3b**.

Complex	E_{HOMO} (eV)	E_{LUMO} (eV)	ΔE_{H-L} (eV)	ΔE (eV)	E_{em} (eV)	λ_{em} (nm)
2b	−6.03	−2.44	3.59	2.71	2.42	512
2b'	−5.98	−2.50	3.48	2.62	2.33	532
2b''	−5.95	−2.48	3.47	2.60	2.30	538
3b	−5.63	−2.34	3.29	2.43	2.16	575
3b'	−5.65	−2.38	3.27	2.40	2.13	582

Adding nitrogen atoms to the ancillary ligand

B3LYP/(6-31G**+LANL2DZ) calculations were performed on complexes **4a-c** (Chart 2). These complexes incorporate 2-phenyl-pyridine as the cyclometallating C^N ligand and a 2-azolyl-pyridine with 2 (**4a**), 3 (**4b**) and 4 (**4c**) nitrogen atoms in the azole ring as the ancillary N^N ligand. The goal was to check the effect of increasing the number of nitrogen atoms in the emission energy. The complexes selected for the study correspond to those in which, based on the results of the previous section, the effect of adding nitrogen atoms is expected to be greater, i. e., those with a nitrogen atom in position 2 linking the azole ring to the pyridine.
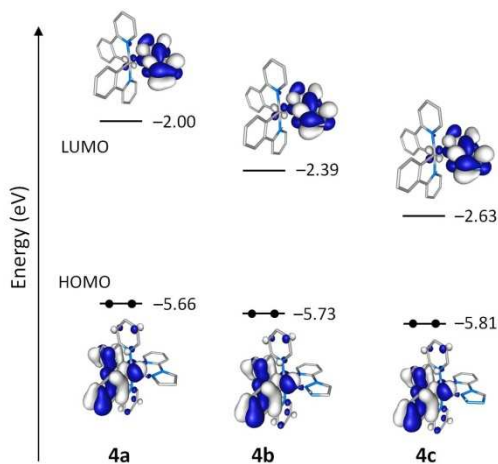
Fig. 4 Schematic representation showing the isovalue contours (±0.03 a.u.) and the energy values (in eV) calculated for the frontier molecular orbitals of complexes **4a-c**. Hydrogen atoms are omitted.

Fig. 4 displays the frontier MOs calculated for complexes **4a-c** at the optimized equilibrium geometry of the ground state. The topology of the MOs is the same obtained for complexes **2a-c** (Fig. 1) and **3a-c** (Fig. 3) with the HOMO centered on the cyclometallating ligands and the d_π orbitals of Ir(III), and the LUMO located on the ancillary ligand. As expected, the energy of both orbitals lowers as the number of nitrogen atoms in the azole ring increases. However, and in contrast with what was found for **2a-c** and **3a-c**, the stabilization is much greater for the LUMO than for the HOMO in complexes **4a-c** (Fig. 4). This effect is due to the fact that the azole ring with an increasing number of nitrogen atoms is now incorporated in the ancillary ligand where the LUMO is located and has a small influence on the HOMO. As a consequence, the HOMO−LUMO gap decreases gradually along the series **4a** (3.66 eV), **4b** (3.34 eV) and **4c** (3.17 eV). Therefore, compared to **2a-c** and **3a-c**, the addition of nitrogen atoms to the azole ring has a completely different effect on complexes **4a-c**, for which a red shift of the emission has to be expected as the number of nitrogen atoms of the azole increases.

Table 5 Lowest triplet excited states calculated at the TD-DFT B3LYP/(6-31G**+LANL2DZ) level for complexes **4a**, **4b**, and **4c** in Acetonitrile solution. Vertical excitation energies (E), dominant monoexcitations with contributions (within parentheses) greater than 20%, and description of the excited state are summarized. H and L denote HOMO and LUMO, respectively.

Complex	State	E (eV)	Monoexcitations	Description[b]
4a	T_1	2.77	H → L+1 (65)	$^3LC/^3MLCT$
	T_2	2.81	H → L+2 (53)	$^3LC/^3MLCT$
			H−1 → L+1 (24)	$^3LC/^3MLCT$
	T_3	2.94	H → L (97)	$^3MLCT/^3LLCT$
4b	T_1	2.60	H → L (98)	$^3MLCT/^3LLCT$
	T_2	2.78	H → L+1 (60)	$^3LC/^3MLCT$
	T_3	2.82	H → L+2 (41)	$^3LC/^3MLCT$
			H−1 → L+1 (23)	$^3LC/^3MLCT$
4c	T_1	2.44	H → L (98)	$^3MLCT/^3LLCT$
	T_2	2.79	H → L+1 (52)	$^3LC/^3MLCT$
	T_3	2.83	H → L+3 (36)	$^3LC/^3MLCT$
			H−1 → L+1 (22)	$^3LC/^3MLCT$

As previously done for **2** and **3**, TD-DFT calculations were performed to determine the nature and relative energy of the lowest-lying triplet excited states of **4a-c** (Table 5). The MLCT/LLCT triplet state originating in the HOMO → LUMO excitation appears at lower energies as we progress in the series **4a** (2.94 eV) > **4b** (2.60 eV) > **4c** (2.44 eV) in good agreement with the trend expected from the HOMO−LUMO gap. Not far from this state, at around 2.80 eV, two LC/MLCT triplet states centered on the cyclometallating-Ir(III) environment are found. The energy of these states remains mostly constant along the series because they have no significant contribution from MOs centered on the ancillary ligand where nitrogen atoms are added. However, it is worth noting that for complex **4a** the HOMO → LUMO triplet corresponds to the T_3 state and is computed higher in energy than the LC/MLCT triplets. In **4b** and **4c**, the stabilization effect of the nitrogen atoms is high enough to place the HOMO → LUMO MLCT/LLCT state as the first triplet state (T_1), as it was found for **2a-c** and **3a-c**.
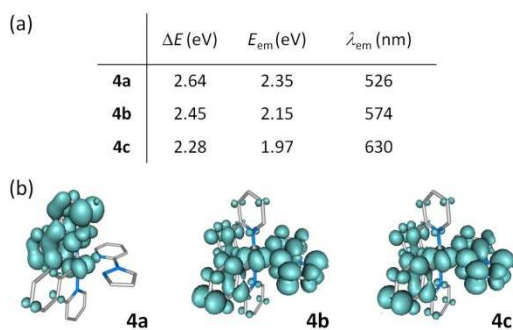
Fig. 5 a) Adiabatic energy difference (ΔE) between S_0 and T_1 and emission energy (E_{em} and λ_{em}) from T_1 computed for complexes **4a**-**c**. b) Unpaired-electron spin-density contours (0.002 au) calculated for the fully relaxed T_1 state.

Fig. 5 summarizes the photophysical properties calculated for complexes **4a-c** after fully-relaxing the geometry of the T_1 state using the UB3LYP approach, together with the corresponding spin density distributions. UB3LYP calculations fully support the results obtained from the TD-DFT study. The emission energy undergoes a red shift in passing from **4a** (2.35 eV) to **4c** (1.97 eV). According to the spin-density distribution, the lowest-energy triplet of **4b** and **4c** has a MLCT/LLCT nature and results from the HOMO → LUMO excitation. In contrast, as predicted by the TD-DFT study, the spin-density distribution calculated for the first triplet of **4a** is mainly centered on one of the cyclometallating ligands (1.65 unpaired electrons) with some contribution from the iridium atom (0.29e) and T_1 has a predominant LC nature with some MLCT character. The photoluminescence spectrum recorded for **4a** presents a marked vibronic structure at room temperature that becomes more accentuated when the spectrum is registered at low temperatures.[53] These features point to an emissive excited state with predominantly $\pi-\pi^*$ character, which is in good agreement with the ^{3}LC C^N description here predicted for the T_1 state of **4a**. It has to be mentioned that He et al. studied complex **4a** at the same theoretical level we use here but without including the effect of the solvent in the calculations.[53] The TD-DFT calculations reported by He et al. indicated that the HOMO → LUMO MLCT/LLCT state was the lowest-lying triplet (2.43 eV) and was located 0.27 eV below the first LC triplet. This assignment was in conflict with the experimental spectrum, which pointed to an emitting ^{3}LC state. The inclusion of solvent effects, as performed in this work, leads to a destabilization of the low-energy triplets of **4a**. However, while the LC triplets undergo a slight destabilization relative to S_0, passing from 2.70 and 2.75 eV in gas phase to 2.77 and 2.81 eV in acetonitrile, the HOMO → LUMO MLCT/LLCT state experiments a large destabilization from 2.43 to 2.93 eV and lies higher in energy than the LC triplets. Solvent effects are therefore needed to obtain a description of the emitting triplet in good agreement with the experimental evidences.

Conclusions

The emission energies of different series of cationic Iridium(III) [Ir(C^N)$_2$(N^N)]$^+$ complexes incorporating azole rings in both the cyclometallating C^N and the ancillary N^N ligands have been theoretically investigated. The structure of the ligands has been modified by changing the number (from 2 to 4) and position of the nitrogen atoms in the azole ring. Calculations show that an increment in the number of nitrogen atoms modifies the relative stability of the frontier MOs leading to changes in the HOMO−LUMO gap and in the energy of the lowest-lying triplet excited states from which emission takes place. When the azole ring forms part of the C^N ligands, the increment in the number of nitrogen atoms stabilizes the HOMO in a higher degree than the LUMO and leads to an enlargement of the HOMO−LUMO energy gap. As a result, a gradual blue shift of the emission wavelength is obtained as the number of nitrogen atoms in the azole ring grows. In contrast, when the azole ring is incorporated in the ancillary N^N ligand, the stabilization of the LUMO is greater than that of the HOMO and, as a consequence, the HOMO−LUMO gap narrows and the emission wavelength gradually shifts to the red.

Calculations also show that the position in which the nitrogen atoms are placed in the azole ring plays a relevant role in determining the emission energy. For complexes bearing a phenyl-azole as the C^N ligand, it has been shown that the largest effect is associated with the azole position to which the phenyl ring is linked. Complexes in which the linking position is occupied by a nitrogen atom present a larger HOMO−LUMO gap and a significant blue-shifted emission (~0.3 eV) compared to those with the same number of nitrogen atoms in the azole ring and bearing a carbon atom in that position. Therefore, when comparing the emission properties of azole-based [Ir(C^N)$_2$(N^N)]$^+$ complexes, not only the number of nitrogen atoms but also the nature of the atom (nitrogen or carbon) to which the aryl group is connected to should be taken into account. In a coherent series of complexes, where the nature of the atom in the linking position is maintained, a gradual shift of the emission wavelength is always found as the number of nitrogen atoms in the azole ring increases and, as long as the azole ring is in the C^N ligands, the shift will be to bluer wavelengths.

Finally, it should be emphasized that solvent effects have to be included in the theoretical calculation to get a proper description of the distribution of the excited states and, in some cases, of the electronic nature of the emitting state.

Notes and references

^{a} *Instituto de Ciencia Molecular, Universidad de Valencia, Catedrático José Beltrán 2, 46980 Paterna, Spain. E-mail: enrique.orti@uv.es.*

Electronic Supplementary Information (ESI) available: Optimized geometries (*xyz* coordinates) of the electronic ground state (S_0) and lowest-energy triplet (T_1) of all the complexes studied.

Dalton Transactions Accepted Manuscript

1 Q. B. Pei, G. Yu, C. Zhang, Y. Yang and A. J. Heeger, *Science*, 1995, **269**, 1086.

2 J. D. Slinker, D. Bernards, P. L. Houston, H. D. Abruña, S. Bernhard and G. G. Malliaras, *Chem. Commun.*, 2003, 2392.

3 J. D. Slinker, J. A. DeFranco, M. J. Jaquith, W. R. Silveira, Y. Zhong, J. M. Moran-Mirabal, H. G. Graighead, H. D. Abruña, J. A. Marohn and G. G. Malliaras, *Nature Mater.*, 2007, **6**, 894.

4 P. Matyba, K. Maturova, M. Kemerink, N. D. Robinson and L. Edman, *Nature Materials*, 2009, **8**, 672.

5 M. Stössel, J. Staudigel, F. Steuber, J. Simmerer and A. Winnacker, *Appl. Phys. A* 1999, **68**, 387.

6 R. D. Costa, E. Ortí, H. J. Bolink, F. Monti, G. Accorsi and N. Armaroli, *Angew. Chem. Int. Ed.* 2012, **51**, 8178.

7 L. He, L. Duan, J. Qiao, D. Zhang, L. Wang and Y. Qiu, *Appl. Phys. A*, 2010, **100**, 1035.

8 S. van Reenen, P. Matyba, A. Dzwilewski, R. A. J. Janssen, L. Edman and M. Kemerink, *J. Am. Chem. Soc.*, 2010, **132**, 13776.

9 M. Lenes, G. García-Belmonte, D. Tordera, A. Pertegás, J. Bisquert and H. J. Bolink, *Adv. Funct. Mater.*, 2011, **21**, 1581.

10 Q. Pei, Yang, G. Yu, C. Zhang and A. J. Heeger, *J. Am. Chem. Soc.*, 1996, **118**, 3922.

11 S. Ladouceur and E. Zysman-Colman, *Eur. J. Inorg. Chem.*, 2013, **17**, 2985.

12 R. D. Costa, E. Ortí, H. J. Bolink, S. Graber, S. Schaffner, M. Neuburger, C. E. Housecroft and E. C. Constable, *Adv. Funct. Mater.* 2009, **19**, 3456.

13 J. Wang, F. Zhang, J. Zhang, W. Tang, A. Tang, H. Peng, Z. Xu, F. Teng and Y. Wang, *J. Photochem. Photobiol. C*, 2013, **17**, 69.

14 T. Hu, L. He, L. Duan and Y. Qiu, *J. Mater. Chem.*,2012, **10**,4206.

15 A. F. Rausch, M. E. Thompson and H. Yersin, *J. Phys. Chem. A*, 2009, **113**, 5927.

16 C.-H. Yang, S.-W. Li, Y. Chi, Y.-M. Cheng, Y.-S. Yeh, P.-T. Chou, G.-H. Lee, C.-H. Wang and C.-F. Shu, *Inorg. Chem.*, 2005, **44**, 7770.

17 T. Sajoto, P. I. Djurovich, A. B. Tamayo, J. Oxgaard, W. A. Goddard and M. E. Thompson, *J. Am. Chem. Soc.*, 2009, **131**, 9813.

18 V. N. Kozhevnikov, K. Dahms and M. R. Bryce, *J. Org.Chem.*, 2011, **76**, 5143.

19 R. D. Costa, F. Monti, G. Accorsi, A. Barbieri, H. J. Bolink, E. Ortí and N. Armaroli, *Inorg. Chem.*, 2011, **50**, 7229.

20 N. M. Shavaleev, F. Monti, R. D. Costa, R. Scopelliti, H. J. Bolink, E. Ortí, G. Accorsi, N. Armaroli, E. Baranoff, M. Gratzel and M. K. Nazeeruddin, *Inorg. Chem.*, 2012, **51**, 2263.

21 N. M. Shavaleev, F. Monti, R. Scopelliti, N. Armaroli, M. Gratzel and M. K. Nazeeruddin, *Organometallics*, 2012, **31**, 6288.

22 J. M. Fernández-Hernández, S. Ladouceur, Y. Shen, A. Iordache, X. Wang, L. Donato, S. Gallagher-Duval, M. de Anda Villa, J. D. Slinker, L. De Cola and E. Zysman-Colman, *J. Mater. Chem. C*, 2013, **1**, 7440.

23 C.-H. Yang, M. Mauro, F. Polo, S. Watanabe, I. Muenster, R. Frohlich and L. De Cola, *Chem. Mater.*, 2012, **24**, 3684.

24 N. M. Shavaleev, F. Monti, R. Scopelliti, A. Baschieri, L. Sambri, N. Armaroli, M. Gratzel and M. K. Nazeeruddin, *Organometallics*, 2013, **32**, 460.

25 V. V. Grushin, N. Herron, D. D. LeCloux, W. J. Marshall, V. A. Petrov and Y. Wang, *Chem. Commun.*, 2001, 1494.

26 E. W. Thomas and M. M. Cudahy, *J. Org. Chem.*, 1993, **58**, 1623.

27 S. Lamansky, P. I. Djurovich, D. Murphy, F. Abdel-Razzaq, R. Kwong, I. M. Tsyba, M. Bortz, B. Mui, R. Bau and M. E. Thompson, *Inorg. Chem.*, 2001, **40**, 1704.

28 D. Tordera, J. J. Serrano-Pérez, A. Pertegás, E. Ortí, H. J. Bolink, E. Baranoff, Md. K. Nazeeruddin and Julien Frey, *Chem. Mater.*, 2013, **25**, 3391.

29 A. B. Tamayo, S. Garon, T. Sajoto, P. I. Djurovich, I. M. Tsyba, R. Bau and M. E. Thompson, *Inorg. Chem.*, 2005, **44**, 8723.

30 M.-L. Ho, F.-M. Hwang, P.-N. Chen, Y.-H. Hu, Y.-M. Cheng, K.-S. Chen, G.-H. Lee, Y. Chi and P.-T. Chou, *Org. Biomol. Chem.*, 2006, **4**, 98.

31 L. He, L. Duan, J. Qiao, G. Dong, L. Wang and Y. Qiu, *Chem. Mater.*, 2010, **22**, 3535.

32 E. Baranoff, H. J. Bolink, E. C. Constable, M. Delgado, D. Häussinger, C. E. Housecroft, M. K. Nazeeruddin, M. Neuburger, E. Ortí, G. E. Schneider, D. Tordera, R. M. Walliser, and J. A. Zampese, *Dalton Trans.* 2013, **42**,1073

33 E. Baranoff, S. Fantacci, F. De Angelis, X. Zhang, R. Scopelliti, M. Gratzel and M. K. Nazeeruddin, *Inorg. Chem.*, 2011, **50**, 451.

34 W.-Y. Lai, J. W. Levell, A. C. Jackson, S.-C. Lo, P. V. Bernhardt, I. D. W. Samuel and P. L. Burn, *Macromolecules*, 2010, **43**, 6986.

35 B. Beyer, C. Ulbricht, D. Escudero, C. Friebe, A. Winter, L. González and U. S. Schubert, *Organometallics*, 2009, **28**, 5478.

36 S. Ladouceur, D. Fortin and E. Zysman-Colman, *Inorg. Chem.*, 2011, **50**, 11514.

37 J. M. Fernández-Hernández, C.-H. Yang, J. I. Beltrán, V. Lemaur, F. Polo, R. Frohlich, J. Cornil and L. De Cola, *J. Am. Chem. Soc.*, 2011, **133**, 10543.

38 M. de Barros e Silva Botelho, J. M. Fernández-Hernández, T. B. de Queiroz, H. Eckert, L. De Cola and A. S. S. de Camargo, *J. Mater. Chem.*, 2011, **21**, 8829.

39 J. M. Fernández-Hernández, J. I. Beltrán, V. Lemaur, M.-D. Gálvez-López, C.-H. Chien, F. Polo, E. Orselli, R. Frohlich, J. Cornil and L. De Cola, *Inorg. Chem.*, 2013, **52**, 1812.

40 L. Donato, P. Abel and E. Zysman-Colman, *Dalton Trans.*, 2013, **42**, 8402.

41 F. Monti, A. Baschieri, I. Gualandi, J. J. Serrano-Pérez, J. M. Junquera-Hernández, D. Tonelli, A. Mazzanti, S. Muzzioli, S. Stagni, C. Roldán-Carmona, A. Pertegás, H. J. Bolink, E. Ortí, L. Sambri and N. Armaroli, *Inorg. Chem.*, 2014, **53**, 7709.

42 *Gaussian 09, Revision C.01*, M. J. Frisch, G. W. Trucks, H. B. Schlegel, G. E. Scuseria, M. A. Robb, J. R. Cheeseman, G. Scalmani, V. Barone, B. Mennucci, G. A. Petersson, H. Nakatsuji, M. Caricato, X. Li, H. P. Hratchian, A. F. Izmaylov, J. Bloino, G. Zheng, J. L. Sonnenberg, M. Hada, M. Ehara, K. Toyota, R. Fukuda, J. Hasegawa, M. Ishida, T. Nakajima, Y. Honda, O. Kitao, H. Nakai, T. Vreven, J. Montgomery, J. A., J. E. Peralta, F. Ogliaro, M. Bearpark, J. J. Heyd, E. Brothers, K. N. Kudin, V. N. Staroverov, T. Keith, R. Kobayashi, J. Normand, K. Raghavachari, A. Rendell, J. C. Burant, S. S. Iyengar, J. Tomasi, M. Cossi, N. Rega, J. M. Millam, M. Klene, J. E. Knox, J. B. Cross, V. Bakken, C. Adamo, J. Jaramillo, R. Gomperts, R. E. Stratmann, O. Yazyev, A. J. Austin, R. Cammi, C. Pomelli, J. W. Ochterski, R. L. Martin, K. Morokuma, V. G. Zakrzewski, G. A. Voth, P. Salvador, J. J. Dannenberg, S. Dapprich, A. D. Daniels, Ö. Farkas, J. B. Foresman, J.

V. Ortiz, J. Cioslowski and D. J. Fox, *Gaussian, Inc., Wallingford CT,* 2010.

43   A. D. Becke, *J. Chem. Phys.*, 1993, **98**, 5648.

44   C. Lee, W. Yang and R. G. Parr, *Phys. Rev. B*, 1988, **37**, 785.

45   M. M. Francl, W. J. Pietro, W. J. Hehre, J. S. Binkley, M. S. Gordon, D. J. Defrees and J. A. Pople, *J. Chem. Phys.*, 1982, **77**, 3654.

46   P. J. Hay and W. R. Wadt, *J. Chem. Phys.*, 1985, **82**, 299.

47   J. Tomasi and M. Persico, *Chem. Rev.*, 1994, **94**, 2027.

48   C. S. Cramer and D. G. Truhlar, *Solvent Effects and Chemical Reactivity* Kluwer, Dordrecht, 1996, pp. 1–80.

49   J. Tomasi, B. Mennucci and R. Cammi, *Chem. Rev.*, 2005, **105**, 2999.

50   K. Nozaki, K. Takamori, Y. Nakatsugawa and T. Ohno, *Inorg. Chem.*, 2006, **45**,6161.

51   S. B. Meier, W. Sarfert, J. M. Junquera-Hernández, M. Delgado, D. Tordera. E. Ortí, H. J. Bolink, F. Kessler, R. Scopelliti, M. Grätzel and M. K. Nazeeruddin*, J. Mater. Chem. C*, 2013, **1**, 58.

52   F. De Angelis, S. Fantacci, N. Evans, C. Klein, S. M. Zakeeruddin, J.-E. Moser, K. Kalyanasundaram, H. J. Bolink, M. Grätzel and M. K. Nazeeruddin, *Inorg. Chem.*, 2007, **46**, 5989.

53   L. He, L. Duan, J. Qiao, R. Wang, P. Wei, L. Wang and Y. Qiu, *Adv. Func. Mater.*, 2008, **18**, 2123.

Dalton Transactions Accepted Manuscript

Entry for the Table of Contents

Emission energy of azole-based ionic iridium(III) complexes: A theoretical study

Paula Pla, José M. Junquera-Hernández, Henk J. Bolink and Enrique Ortí*

Instituto de Ciencia Molecular, Universidad de Valencia, Catedrático José Beltrán 2, 46980 Paterna, Spain. E-mail: enrique.orti@uv.es.
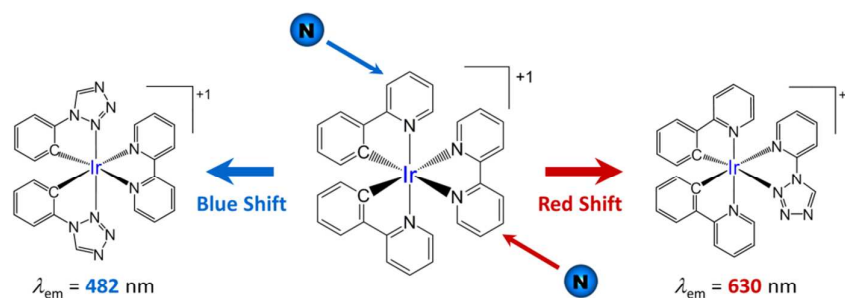
Tuning the emission color of azole-based iridium(III) complexes by changing the number and position of nitrogen atoms in the azole ring.